Vol. 6 • No. 17 • September 4 • 2018

www.advopticalmat.de

ADVANCED OPTICAL MATERIALS

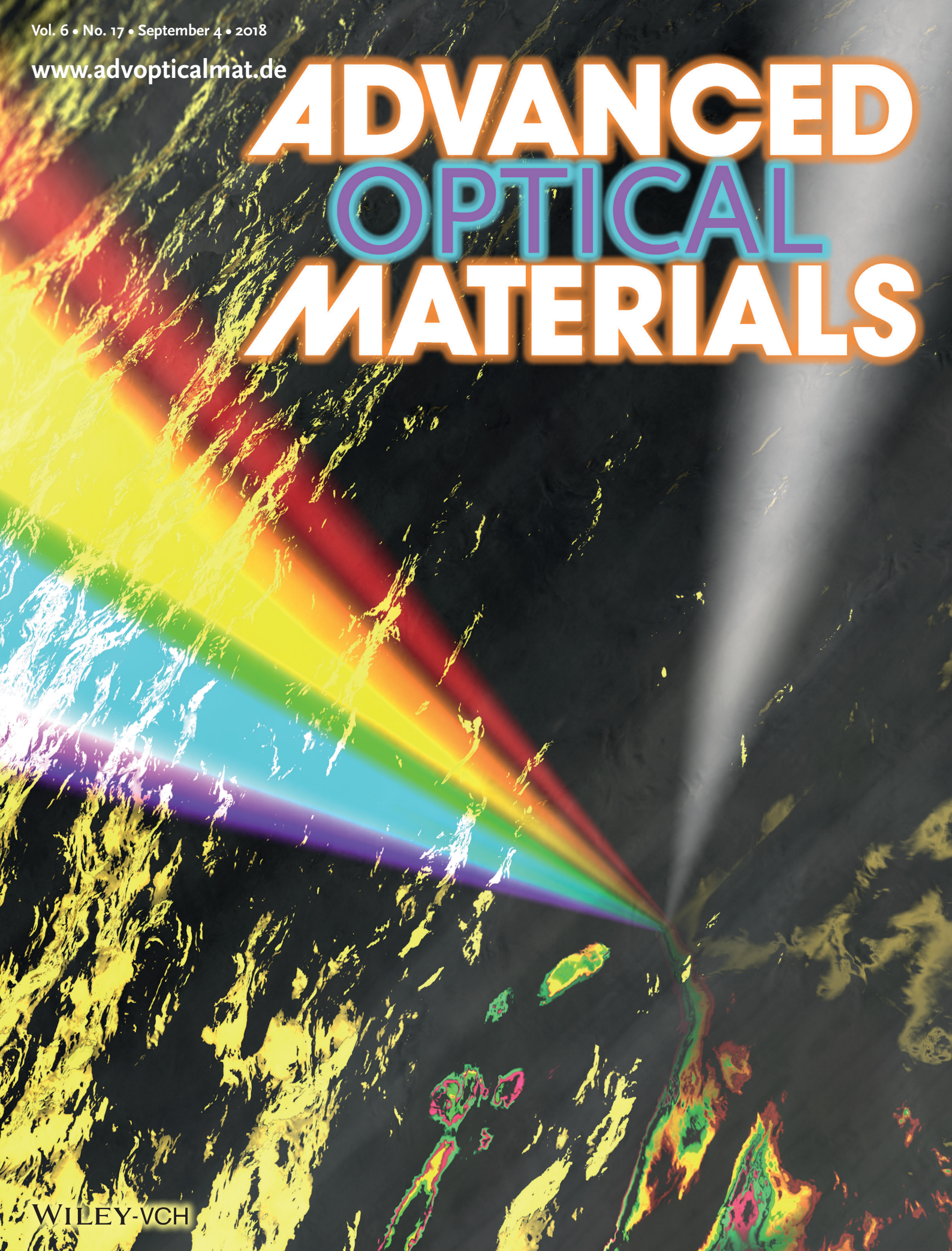

WILEY-VCH

ADVANCED OPTICAL MATERIALS
www.advopticalmat.de

Band Structure Engineering by Alloying for Photonics

*Chen Gong, Alan Kaplan, Zackery A. Benson, David R. Baker, Joshua P. McClure, Alexandre R. Rocha, and Marina S. Leite**

Surface plasmon polaritons (SPPs) enable the deep subwavelength confinement of an electromagnetic field, which can be used in optical devices ranging from sensors to nanoscale lasers. However, the limited number of metals that satisfy the required boundary conditions for SPP propagation in a metal/dielectric interface severely limits its occurrence in the visible range of the electromagnetic spectrum. We introduce the strategy of engineering the band structure of metallic materials by alloying. We experimentally and theoretically establish the control of the dispersion relation in Ag–Au alloys by varying the film chemical composition. Through X-ray photoelectron spectroscopy (XPS) measurements and partial density-of-states calculations we deconvolute the d band contribution of the density-of-states from the valence band spectrum, showing that the shift in energy of the d band follows the surface plasmon resonance change of the alloy. Our density functional theory calculations of the alloys band structure predict the same variation of the threshold of the interband transition, which is in very good agreement with our optical and XPS experiments. By elucidating the correlation between the optical behavior and band structure of alloys, we anticipate the fine control of the optical properties of metallic materials beyond pure metals.

Surface plasmon polaritons (SPPs) are defined as travelling electromagnetic waves at the interface between a metal and a dielectric, resulting from a waveguiding effect that occurs when the wave vectors of both the photons and the surface plasmons match. The subsequent electromagnetic field propagates along the metal–dielectric interface with a much smaller wavelength than the incident light.[1] These characteristics give rise to a strong electric field confinement near the surface, which allows for the manipulation of light at deep sub-wavelengths,[2] leading to a variety of applications including nanolasers,[3] sensors,[4] bioimaging,[5] surface-enhanced Raman spectroscopy,[6,7] color displays,[8] and others.[9–12]

To improve the performance of today's photonic systems, researchers have extensively investigated the fundamental relation between the wave vector and energy of an SPP wave—named dispersion relation. This quantity describes the propagation of light within a material (i.e., medium), extremely relevant for the abovementioned optical devices. Therefore, understanding the dispersion relation can allow the design of optical materials with superior response, ranging from 2D van der Waals to oxides and metals. Concerning 2D materials, it can uncover the origin of tunable polaritons in hyperbolic metamaterials based on graphene and hexagonal boron nitride (h-BN), which is due to the hybridization of SPP and surface phonon polaritons.[13] As another example, by utilizing the band-edge mode of the dispersion relation in metallic nanocavities,[3] lasing with a 200 times enhancement of the spontaneous emission rate of the dye has been reached.[14]

As a class of emerging photonic materials, noble metal alloys with permittivity and localized surface plasmon resonances not achievable by pure metals[9,15,16] have been proposed as alternative candidates for plasmonics[12,17–20] because of their tunable dielectric functions, which make it possible to engineer the alloy composition to attain optical properties that will meet desired resonances. In turn, this tunability could be used to

C. Gong, A. Kaplan, Z. A. Benson, Prof. M. S. Leite
Institute for Research in Electronics and Applied Physics
University of Maryland
College Park, MD 20742, USA
E-mail: mleite@umd.edu
C. Gong, A. Kaplan, Prof. M. S. Leite
Department of Materials Science and Engineering
University of Maryland
College Park, MD 20742, USA
The ORCID identification number(s) for the author(s) of this article can be found under https://doi.org/10.1002/adom.201800218.
Z. A. Benson
Department of Physics
University of Maryland
College Park, MD 20742, USA
Dr. D. R. Baker, Dr. J. P. McClure
Sensors and Electron Devices Directorate
U.S. Army Research Laboratory
Adelphi, MD 20783, USA
Prof. A. R. Rocha
Instituto de Física Teórica (IFT)
Universidade Estadual Paulista (UNESP)
São Paulo, SP 01140-070, Brazil

DOI: 10.1002/adom.201800218

improve the performance of devices for a variety of applications, such as perfect absorbers,[21] photovoltaics,[22] hydrogen storage,[23] metallurgy,[24] catalysis,[25] and electrocatalysis.[26–28] However, in contrast to the well-investigated dispersion relation of pure noble metals (Ag and Au),[29–34] the dispersion of SPPs for Ag–Au alloys has rarely been explored.[35] Additionally, the correlations between the effect of alloying on the optical dispersion relation, the threshold of the interband transition, and the new material's band structure are still not well understood.

In this paper, we experimentally and theoretically demonstrate the SPP dispersion relation of Ag–Au alloyed thin films (Ag_xAu_{1-x}) and explain the origin of their behavior by combining optical and X-ray photoelectron spectroscopy (XPS) measurements with density functional theory (DFT) band structure calculations. The Ag_xAu_{1-x} alloy represents an ideal model system to establish the correlation between the material dispersion relation and its electronic band structure as a solid solution is formed for the entire chemical composition range.[36] We map the reflectivity as a function of wavelength and angle of incidence for Ag_xAu_{1-x} films using the Kretschmann configuration,[37] and find that the dispersion relation can be engineered by changing the alloy chemical composition. The physical origin of the observed optical response is correlated to the valence band spectra (VBS) obtained by XPS measurements. In particular, the VBS in conjunction with partial density-of-states (DOS) calculations reveal a dependence of the binding energy onset of the d band and the corresponding energy of the transmission resonance peak for a given alloy. This dependence indicates the relation between the threshold of the interband transition and the energy of the d band. To underpin this relation, we further calculate the band structure for each alloy by DFT to assess the regions in reciprocal space where optical transitions occur. A similar change for the interband transition is determined, agreeing remarkably well with our optical and XPS measurements. Further, we reveal the nonlinear specific contribution of each metal to the band structure of the alloys. Overall, our results provide fundamental insight into the origin of the surface plasmon modes in Ag_xAu_{1-x} alloys and show that the band structure can be engineered upon changing the alloy's chemical composition. We anticipate the combined experimental + computational approach presented here to be extended to other materials, including nonmetallic ones. Ultimately, their optical behavior is influenced by the electronic properties (e.g., density of carriers), which urgently requires a combined analysis. When merged with a combinatorial materials screening, this paradigm can offer a library of emerging materials for photonics.

We fabricate the alloyed metallic thin films by cosputtering Ag and Au onto glass microscope slides (see Methods in the Supporting Information). The samples are rotated during deposition to ensure uniform chemical composition, confirmed by energy-dispersive X-ray spectroscopy (see details in Figure S1 and Table S1 of the Supporting Information). To evaluate the macroscopic optical properties, we measure transmission spectra for each sample, as shown in **Figure 1**. The experimental transmission peaks in Figure 1a

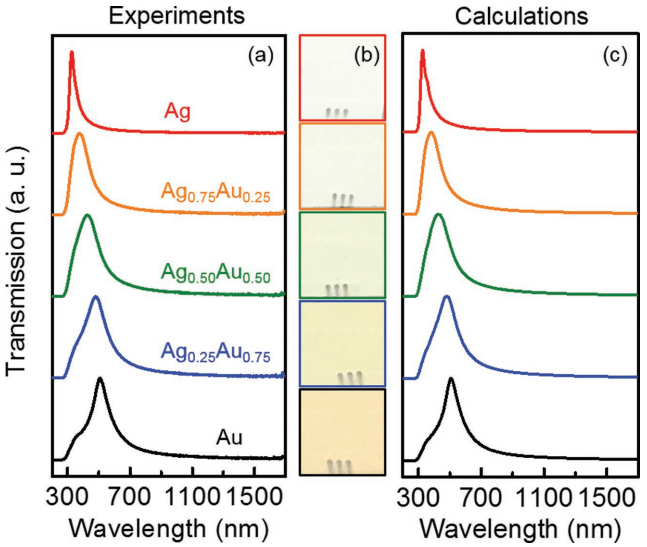

Figure 1. a) Measured transmission spectra of Ag_xAu_{1-x} alloyed thin films. b) Photographs of the alloyed films on glass substrates. c) Calculated transmission spectra using Fresnel equations. Film nominal thickness: 50 nm. Sample size: 2.54 × 2.54 cm^2.

indicate the plasmonic resonances of the films. These peaks shift from 325 nm (pure Ag), to 375 nm ($Ag_{0.75}Au_{0.25}$), to 425 nm ($Ag_{0.50}Au_{0.50}$), to 480 nm ($Ag_{0.25}Au_{0.75}$), to 510 nm (pure Au), indicating the change of the optical response upon varying the chemical composition. These measurements agree with the color change of the sample (see photographs in Figure 1b). Further, we use the Fresnel equations[38] to calculate the transmission of the thin films. The spectra in Figure 1c show excellent agreement between our calculations and the experimentally determined values (also see Figure S2 of the Supporting Information). The trend seen on the peak broadening with increasing Au content happens because the interband transitions at both Γ and R critical points occur at different energies, 2.5 eV and 4.0 eV, respectively. As a result, the transmission peak contains both contributions (at 310 and 496 nm), which are partially overlaid in the optical measurement. By contrast, for Ag these transitions occur at a degenerate energy level: 4.0 eV.[39] Here the permittivity and the film thicknesses (inputs of our calculation) are determined by ellipsometry measurements (see Table S1 and Figure S3 of the Supporting Information).

One approach to assess the dispersion relation of the SPP for the Ag_xAu_{1-x} alloys is by measuring the reflectivity of the films. Here, we use the Kretschmann configuration[37] to provide sufficient momentum to excite SPPs.[40] In our setup, the laser passes through a fused silica prism, which is attached to the glass substrate using an index matching liquid. The ratio of the reflected power to the incident power is then recorded at each wavelength and incident angle to obtain the reflectivity. **Figure 2** displays the reflectivity maps for all Ag_xAu_{1-x} alloyed thin films. The blue narrow band in Figure 2a–e shows reflectivity damping originating from the excitation of leaky modes due to destructive interference of reflected and transmitted light when using prism coupling.[41] Our measurements show that as the Au content increases, the SPP band broadens. For

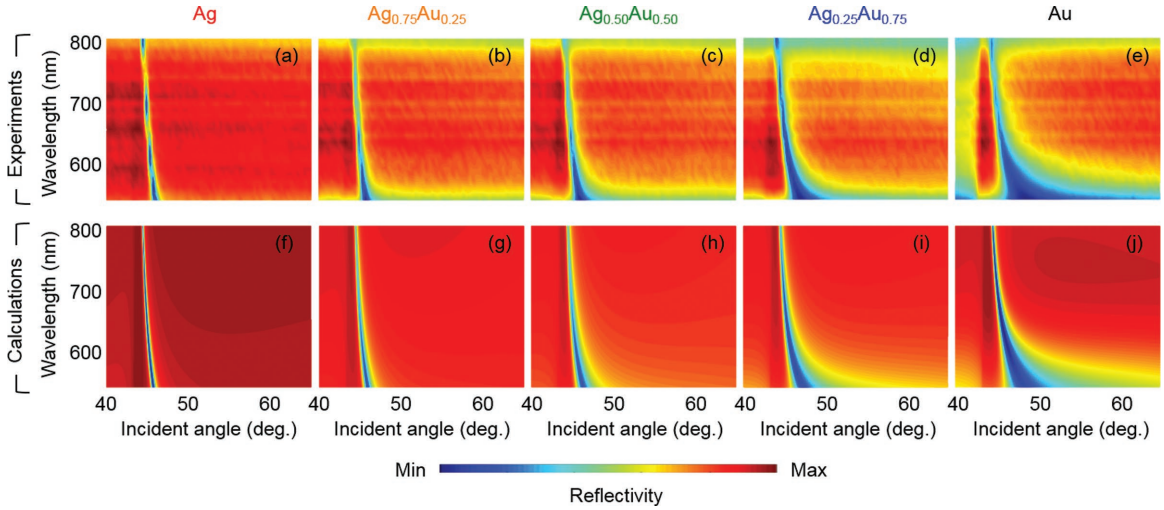

Figure 2. a–e) Measured and f–j) calculated reflectivity maps for Ag_xAu_{1-x} alloyed thin films. The reflectivity is recorded by dividing the reflected power over the power of the incident light. Transfer matrix method is adopted using the experimentally determined permittivity and thickness for each metal and alloy as the inputs.

example, at 600 nm the full-width-half-maximum of the band is 0.5° for pure Ag and 1.9° for pure Au. The physical origin of the bandwidth broadening as the Au content increases is also due to the fact that the interband transition for this metal occurs at 2.5 and 4.0 eV for Γ and R, respectively. The change of the bandwidth for SPP modes provides a tunable optical sensitivity while the chemical stability is kept by the use of Ag–Au alloys.[42] In addition, our experiment has excellent agreement with the theoretical calculations using the transfer matrix method,[43] as shown in Figure 2f–j. The position and intensity of the band, as well as the critical angle (corresponding to the max reflection), match well between the measurements and calculations. To optimize for the largest attenuation of reflection power, the films are fabricated with a 50 nm nominal thickness as per critical coupling when using the Kretschmann configuration (see Table S1 of the Supporting Information for the experimentally determined thicknesses).[40]

Figure 3 provides the dispersion relation for the Ag_xAu_{1-x} alloys obtained from the SPP reflectivity measurements. The wavelength of the light and the incident angle are converted to energy and wave vector, respectively, using the following equations

$$E = \frac{hc}{\lambda} \tag{1}$$

$$k = \sqrt{\varepsilon_{\text{prism}}}\,\frac{f}{c}\sin\theta \tag{2}$$

where E is the energy of the incident light, h is Planck's constant, c is the speed of the light in vacuum, λ is the wavelength

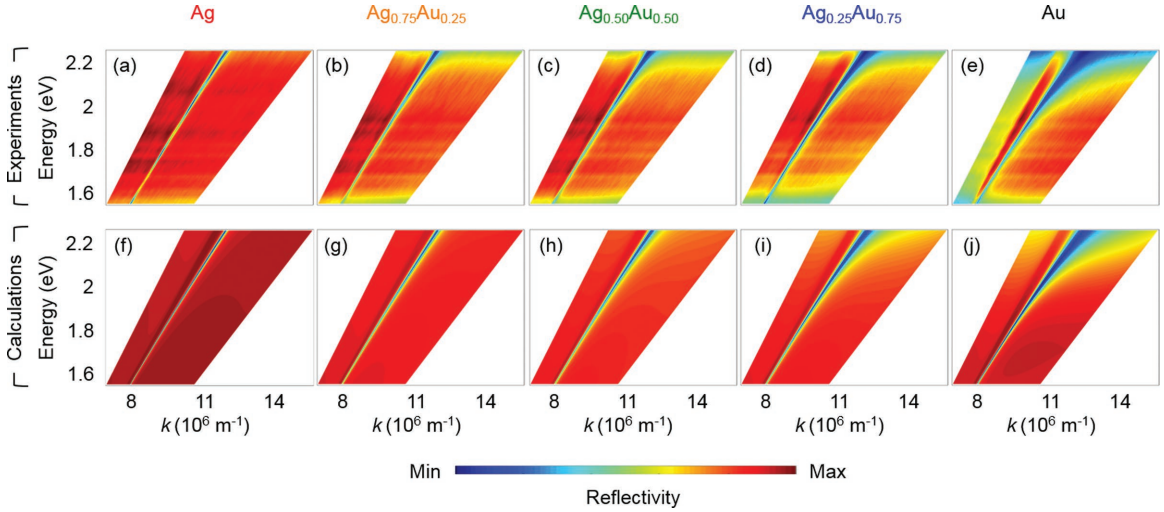

Figure 3. a–e) Measured and f–j) calculated dispersion relation for Ag_xAu_{1-x} alloys. The color refers to the reflectivity at each wave vector k and energy. The minimum reflectivity corresponds to the excitation of surface plasmon polaritons (SPP).

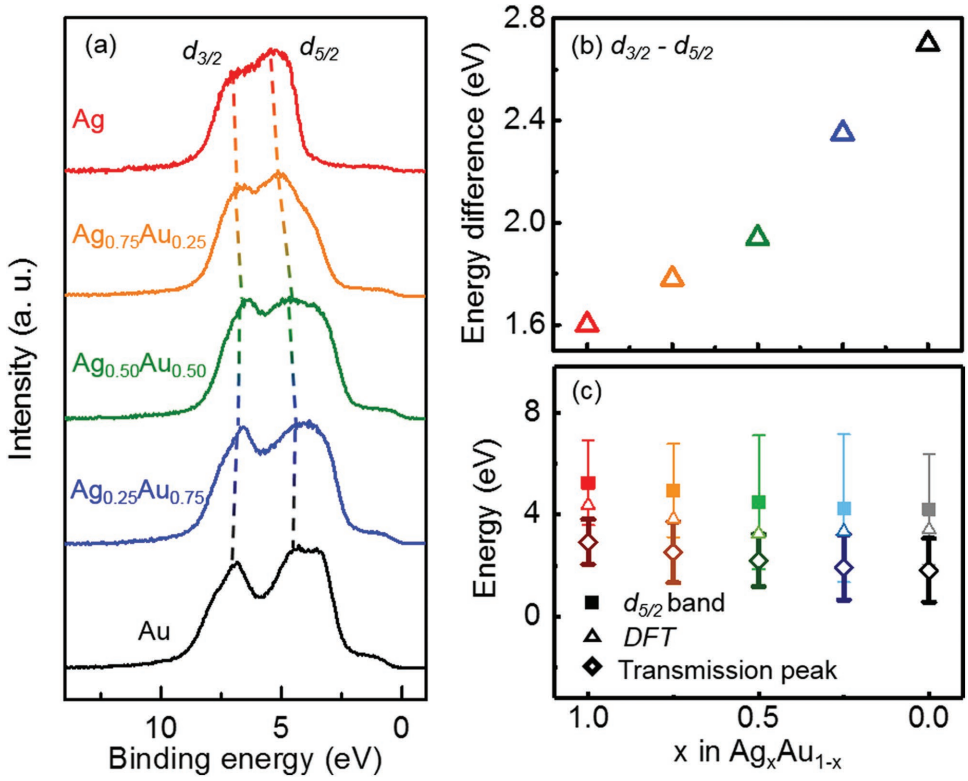

Figure 4. a) Valence band spectra of Ag_xAu_{1-x} alloyed thin films obtained by XPS. Dashed lines show the peak shift for $d_{3/2}$ and $d_{5/2}$, where the $d_{3/2}$ and $d_{5/2}$ peaks are fit by Gaussian functions. b) Energy difference between $d_{3/2}$ and $d_{5/2}$ for each alloy. c) Peak energy of $d_{5/2}$ band (solid squares), transmission measurements (hollow diamonds), and the value of the interband transition determined by DFT (hollow triangle). The error bars refer to the bandwidth of $d_{5/2}$ and transmission peak, which is determined by the lower and higher energy values at 5% of its height.

of the incident light, k is the wave vector, ε_{prism} is the permittivity of the fused silica prism,[44] f is the frequency, and θ is the incident angle. The intensity in the dispersion map corresponds to the reflectivity at each E and k. Figure 3a shows the measured dispersion relation of pure Ag with the antisymmetric plasmon mode resolved.[45] The symmetric mode requires wave vector larger than the prism coupling configuration could offer, thus not accessible.[1] We find that the dispersion relation varies from Ag to Au and it bends toward a lower frequency region for Au-rich alloy ($Ag_{0.25}Au_{0.75}$), which established the control of the dispersion relation by changing the film chemical composition. To corroborate our experiment, we use the experimentally determined permittivity (see Figure S2 of the Supporting Information) to calculate the dispersion maps, as shown in Figure 3f–j. An excellent agreement is achieved between the experiments and calculations, validating our approach to resolve the dispersion.

We experimentally determine the VBS for the alloys with XPS measurements to understand the underlying physics responsible for the change of the surface plasmon resonance, as shown in **Figure 4**. The overall shape of the VBS for Ag_xAu_{1-x} (Figure 4a) agrees with what has been previously reported in the literature.[46,47] Because the electrons of the d band are responsible for the electronic transitions within the visible range, we extract both the $d_{5/2}$ peak and its corresponding split-off $d_{3/2}$ by fitting Gaussian functions to the raw spectra after a Shirley background subtraction (see more details in Methods and Figure S4 of the Supporting Information). From the fitting analysis, a third contributing peak is found along with the $d_{5/2}$ and $d_{3/2}$ components, as evidenced by a shoulder on the lower binding energy side for each alloy. Therefore, the $d_{5/2}$ does not appear at the center of the lower energy peak in the VBS. The three fitted curves change position with alloy composition (see Figure S4 of the Supporting Information). Based on the partial DOS calculation (Figure S5 of the Supporting Information), the three peaks are primarily represented by the d band component (i.e., largest fractional contribution) at binding energies greater than ≈1 eV for each metal or alloy. During the fitting, the peak splitting is variable, and we find that the separation between the $d_{3/2}$ and $d_{5/2}$ bands increases nonlinearly (Figure 4b) as the Au content rises.[48] The width of the d bands has been attributed to several material characteristics,[46,47] but since the overall band structure contains information about additional populated states (i.e., the shoulder peak) care must be taken when identifying the relaxed energy of excited electrons, and ascribing changes in VBS to specific properties. For Ag–Au alloy the width of the $d_{5/2}$ increases with the Au content. This change in the d band of the band structure results in the transmission peak and SPP broadening. The onset binding energy of the $d_{5/2}$ band is specifically investigated because it corresponds to the minimum energy needed for an optical excitation. We define the onset as the lower energy value at 5% of the peak height in order to distinguish the emergence of the peak from the background signal. Figure 4c reveals that this

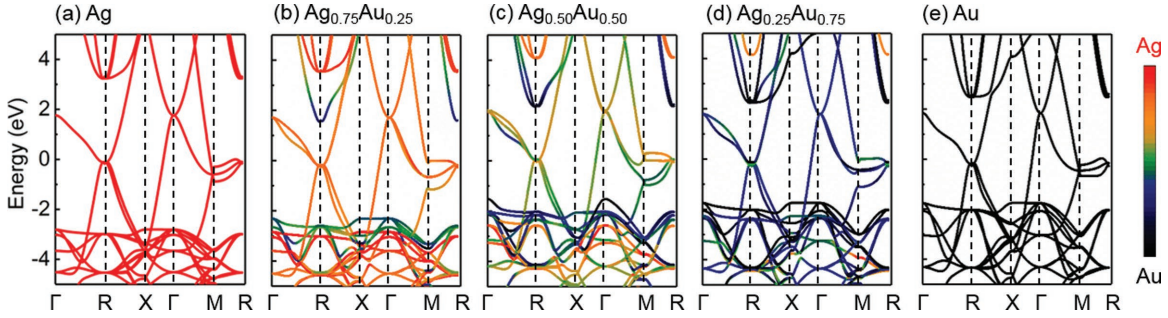

Figure 5. a–e) Density functional theory band structure of Ag_xAu_{1-x} alloys, showing empty states (>0 eV) and the d bands (<0 eV). The color scale refers to the weighted contribution of Ag (red) and Au (black) to each state.

onset aligns well with the transmission measurement (also see Figure S6 of the Supporting Information). For instance, the onset of $d_{5/2}$ for $Ag_{0.50}Au_{0.50}$ is at 2.05 eV and the transmission peak is at 2.40 eV (see Table S2 of the Supporting Information), indicating the origin of the tunability for the interband transition is from the energy shift of the d band. This observation is confirmed by our DFT calculations: the change in the energy for the interband transition is in semi-quantitative agreement with the VBS and optical measurements (see also Figure 4c).

To further investigate the electronic properties of Ag_xAu_{1-x} alloys, we calculate its band structure using DFT,[49] as shown in **Figure 5**. Figure 5a–e displays the band structure of Ag_xAu_{1-x} alloys with the states from the d band below the Fermi level and the empty states above the Fermi level. Here we model all alloys and pure metals as occupying sites in an fcc lattice containing four atoms per unit cell, one in the vertex and three on each side of the cube, as shown in Figure S7 (Supporting Information). Because Ag_xAu_{1-x} forms a solid solution,[36] and the lattice constant remains roughly the same across the whole chemical composition range,[50] four atoms are sufficient to fully describe the unit cells. For $Ag_{0.75}Au_{0.25}$ and $Ag_{0.25}Au_{0.75}$ alloys, the cells are constructed by starting with either Ag or Au in the vertex, and replacing the adjacent atoms in the correct proportion (see Figure S7 of the Supporting Information). For the case of $Ag_{0.50}Au_{0.50}$, the 4-atom model leads to an anisotropic alloy in one particular direction. Nevertheless, the optical transitions occur in the isotropic and symmetric Γ and R points, indicating that the 4-atom cell is a good model for $Ag_{0.5}Au_{0.5}$. While the important transitions within the visible range of the spectrum occur in the X-point in an fcc lattice, which was commonly defined,[39] due to the folding of the bands, the critical point corresponds to Γ point in a 4-atom cell. Our computational study predicts that at the Γ point the position of the d band moves closer to the Fermi level, as the Ag content is reduced, leading to a decrease of the energy gap between the d band and the first empty state (see Figure S8 of the Supporting Information for additional calculations). This reduction indicates that the threshold of the interband transition for Ag_xAu_{1-x} alloys should shift to longer wavelength regions as the Au content rises, agreeing with our optical and VBS measurements (see Figure 4c). Moreover, we identify the contribution of each metal to the overall band structures: the color scale in Figure 5 represents the weight of the pure constituents on each *k*-dependent electronic state (see details in Methods in the Supporting Information). For example, in the $Ag_{0.50}Au_{0.50}$ alloy, Au dominates most of the high-energy states in the d band from −2 to −3 eV, see Figure 5c, while Ag and Au have comparable contributions on other states across all the critical points of the Brillouin Zone (reference to Figure S9 of the Supporting Information for the positions of Γ, R, X, and M). This nonlinear behavior is a direct consequence of the fact that the energy of the d band of Au is ≈1.6 eV higher than Ag.

Here, we report a class of metallic materials based on Ag_xAu_{1-x} with tunable optical response, where we vary the alloy chemical composition to engineer its optical dispersion relation. We attribute the tuning of the SPP dispersion relation to a change of the band structure resulting from alloying, which is theoretically confirmed by DFT calculations. Valence band analysis reveals that the optical resonance variation is directly related to a shift of the d band position, which is tuned by varying the chemical composition. Note that our combined analysis can be expanded to other binary mixtures of metals, such as Au–Cu and Al–Mg, for photonic devices that operate in the near-infrared and ultraviolet–visible range of the electromagnetic spectrum, respectively. By calculating the band structure of combined metallic elements, one can establish a library of possible mixtures with predictive optical/electronic response that are currently not available. In turn, this data could be used as a guideline for identifying the ideal combination of metals for applications ranging from (photo) electrocatalysts to superabsorbers and hot carrier devices.[26,51–53]

In conclusion, we experimentally and theoretically mapped the optical dispersion for Ag_xAu_{1-x} alloyed thin films. By varying the content of Ag and Au, the SPP properties of this metallic material were finely tuned in the visible range of the electromagnetic spectrum. To corroborate our results, we collected the VBS through XPS measurements and deconvoluted the contribution from the d band to the DOS. We found that the shift in energy of the d band aligns very well with the transmission peak of the alloy. The "degeneracy" of the $d_{5/2}$ and $d_{3/2}$ bands is broken, as we increase the content of Au in the film. Further, the band structure calculated by DFT is in good agreement with optical and VBS results when determining the threshold of the interband transition, showing a shift to longer wavelength of the interband transition when Au content increases. Overall, our results helped explain the electronic and optical properties of new metallic materials and provide the potential for the fabrication of scalable, low-cost thin films for surface dispersion engineering. Given that a thorough understanding of the band structure and the optical response allows a systematic method to obtaining metallic materials with tunable optical response,

we foresee that our work will be useful to advance materials' selection for a wide range of applications including, but not limited to, photo-electrochemical water splitting,[54] superabsorbers,[21] metasurfaces,[55] and active plasmonic devices.[56]

Supporting Information

Supporting Information is available from the Wiley Online Library or from the author.

Acknowledgements

The authors gratefully acknowledge E. M. Tennyson, J. M. Howard, and B. R. A. Neves for fruitful discussions, and the Maryland NanoCenter and FabLab for their technical support. The authors thank the financial support from the National Science Foundation Grant No. 16–09414 (DMR), Grant No. HDR1008117 (ADVANCE/UMD program), the 2017–2018 Harry K. Wells Graduate Fellowship, and the ASPIRE-MTech Program at UMD. A.R.R. acknowledges support from FAPESP-Brazil, Grant No. 2017/023172, and Santos Dumont, LNCC-Brazil for computational support.

Conflict of Interest

The authors declare no conflict of interest.

Keywords

band structures, density functional theory, dispersion relations, metal alloys, plasmonics

Received: February 16, 2018
Revised: April 13, 2018
Published online: June 25, 2018

[1] S. A. Maier, *Plasmonics: Fundamentals and Applications*, Springer Science & Business Media, New York, NY **2007**.
[2] A. I. Fernández-Domínguez, F. J. García-Vidal, L. Martín-Moreno, *Nat. Photonics* **2017**, *11*, 8.
[3] D. Wang, A. Yang, W. Wang, Y. Hua, R. D. Schaller, G. C. Schatz, T. W. Odom, *Nat. Nanotechnol.* **2017**, *12*, 889.
[4] J. Homola, S. S. Yee, G. Gauglitz, *Sens. Actuators B* **1999**, *54*, 3.
[5] S. Tu, D. Rioux, J. Perreault, D. Brouard, M. Meunier, *J. Phys. Chem. C* **2017**, *121*, 8944.
[6] S. Nie, S. R. Emory, *Science* **1997**, *275*, 1102.
[7] R. Proietti Zaccaria, F. Bisio, G. Das, G. Maidecchi, M. Caminale, C. D. Vu, F. De Angelis, E. Di Fabrizio, A. Toma, M. Canepa, *ACS Appl. Mater. Interfaces* **2016**, *8*, 8024.
[8] W. L. Barnes, A. Dereux, T. W. Ebbesen, *Nature* **2003**, *424*, 824.
[9] M. B. Ross, J. C. Ku, B. Lee, C. A. Mirkin, G. C. Schatz, *Adv. Mater.* **2016**, *28*, 2790.
[10] H. Y. Hong, J. S. Ha, S.-S. Lee, J. H. Park, *ACS Appl. Mater. Interfaces* **2017**, *9*, 5014.
[11] R. Yu, L. M. Liz-Marzán, F. J. G. de Abajo, *Chem. Soc. Rev.* **2017**, *46*, 6710.
[12] C. Zhang, N. Kinsey, L. Chen, C. Ji, M. Xu, M. Ferrera, X. Pan, V. M. Shalaev, A. Boltasseva, L. J. Guo, *Adv. Mater.* **2017**, *29*, 1605177.
[13] S. Dai, Q. Ma, M. K. Liu, T. Andersen, Z. Fei, M. D. Goldflam, M. Wagner, K. Watanabe, T. Taniguchi, M. Thiemens, F. Keilmann, G. C. A. M. Janssen, S. E. Zhu, P. Jarillo-Herrero, M. M. Fogler, D. N. Basov, *Nat. Nanotechnol.* **2015**, *10*, 682.
[14] W. Zhou, M. Dridi, J. Y. Suh, C. H. Kim, M. R. Wasielewski, G. C. Schatz, T. W. Odom, *Nat. Nanotechnol.* **2013**, *8*, 506.
[15] C. Gong, M. S. Leite, *ACS Photonics* **2016**, *3*, 507.
[16] C. Gong, M. R. S. Dias, G. C. Wessler, J. A. Taillon, L. G. Salamanca-Riba, M. S. Leite, *Adv. Opt. Mater.* **2017**, *5*, 1600568.
[17] O. Peña-Rodríguez, M. Caro, A. Rivera, J. Olivares, J. M. Perlado, A. Caro, *Opt. Mater. Express* **2014**, *4*, 403.
[18] Y. Hashimoto, G. Seniutinas, A. Balčytis, S. Juodkazis, Y. Nishijima, *Sci. Rep.* **2016**, *6*, 25010.
[19] P.-C. Chen, X. Liu, J. L. Hedrick, Z. Xie, S. Wang, Q.-Y. Lin, M. C. Hersam, V. P. Dravid, C. A. Mirkin, *Science* **2016**, *352*, 1565.
[20] Y. Wu, G. Li, C. Cherqui, N. W. Bigelow, N. Thakkar, D. J. Masiello, J. P. Camden, P. D. Rack, *ACS Photonics* **2016**, *3*, 130.
[21] M. R. S. Dias, C. Gong, Z. A. Benson, M. S. Leite, *Adv. Opt. Mater.* **2018**, *6*, 1700830.
[22] M. Xu, J. Feng, Y.-S. Liu, Y. Jin, H.-Y. Wang, H.-B. Sun, *Appl. Phys. Lett.* **2014**, *105*, 160.
[23] Y. Nishijima, S. Shimizu, K. Kurihara, Y. Hashimoto, H. Takahashi, A. Balčytis, G. Seniutinas, S. Okazaki, J. Juodkazyt , T. Iwasa, *Opt. Express* **2017**, *25*, 24081.
[24] A. Herz, M. Friák, D. Rossberg, M. Hentschel, F. Theska, D. Wang, D. Holec, M. Šob, O. Schneeweiss, P. Schaaf, *Appl. Phys. Lett.* **2015**, *107*, 073109.
[25] G. Chen, R. Gao, Y. Zhao, Z. Li, G. I. Waterhouse, R. Shi, J. Zhao, M. Zhang, L. Shang, G. Sheng, *Adv. Mater.* **2017**, *30*, 1704663.
[26] J. Li, H.-M. Yin, X.-B. Li, E. Okunishi, Y.-L. Shen, J. He, Z.-K. Tang, W.-X. Wang, E. Yücelen, C. Li, *Nat. Energy* **2017**, *2*, 17111.
[27] A. Holewinski, J.-C. Idrobo, S. Linic, *Nat. Chem.* **2014**, *6*, 828.
[28] J. Kim, C. W. Roh, S. K. Sahoo, S. Yang, J. Bae, J. W. Han, H. Lee, *Adv. Energy Mater.* **2018**, *8*, 1701476.
[29] T. T. Ehler, L. J. Noe, *Langmuir* **1995**, *11*, 4177.
[30] C. Zhong, K. E. Ballantine, C. Kervick, C. M. Smith, D. Mullarkey, I. Shvets, J. F. Donegan, D. McCloskey, *J. Opt. Soc. Am. B* **2016**, *33*, 566.
[31] M. Ives, T. M. Autry, S. T. Cundiff, G. Nardin, *J. Opt. Soc. Am. B* **2016**, *33*, C17.
[32] G. Schider, J. Krenn, A. Hohenau, H. Ditlbacher, A. Leitner, F. Aussenegg, W. Schaich, I. Puscasu, B. Monacelli, G. Boreman, *Phys. Rev. B* **2003**, *68*, 155427.
[33] B. H. Ong, X. Yuan, S. C. Tjin, J. Zhang, H. M. Ng, *Sens. Actuators, B* **2006**, *114*, 1028.
[34] S. Y. Park, D. Stroud, *Phys. Rev. B* **2004**, *69*, 125418.
[35] Z. Liu, D. Ji, X. Zeng, H. Song, J. Liu, S. Jiang, Q. Gan, *Appl. Phys. Express* **2015**, *8*, 042601.
[36] W. Cao, Y. Chang, J. Zhu, S. Chen, W. Oates, *Intermetallics* **2007**, *15*, 1438.
[37] E. Kretschmann, H. Raether, *Z. Naturforsch. A: Phys. Sci.* **1968**, *23*, 2135.
[38] E. Hecht, *Optics*, Addison-Wesley, Boston, MA **2002**.
[39] D. Rioux, S. Vallières, S. Besner, P. Muñoz, E. Mazur, M. Meunier, *Adv. Opt. Mater.* **2014**, *2*, 176.
[40] O. Pluchery, R. Vayron, K.-M. Van, *Eur. J. Phys.* **2011**, *32*, 585.
[41] H. Raether, *Surface Plasmons on Smooth and Rough Surfaces and on Gratings*, Springer, Berlin **1988**.
[42] C. Gao, Y. Hu, M. Wang, M. Chi, Y. Yin, *J. Am. Chem. Soc.* **2014**, *136*, 7474.
[43] J. D. Jackson, *Classical Electrodynamics*, John Wiley & Sons, Hoboken, NJ **2007**.
[44] I. Malitson, *J. Opt. Soc. Am.* **1965**, *55*, 1205.
[45] J. Dionne, L. Sweatlock, H. Atwater, A. Polman, *Phys. Rev. B* **2005**, *72*, 075405.
[46] T.-U. Nahm, S.-J. Oh, S.-M. Chung, *J. Electron Spectrosc. Relat. Phenom.* **1996**, *78*, 127.
[47] T. Sham, A. Bzowski, M. Kuhn, C. Tyson, *Solid State Commun.* **1991**, *80*, 29.

[48] A. Bzowski, M. Kuhn, T. Sham, J. Rodriguez, J. Hrbek, *Phys. Rev. B* **1999**, *59*, 13379.
[49] J. M. Soler, E. Artacho, J. D. Gale, A. García, J. Junquera, P. Ordejón, D. Sánchez-Portal, *J. Phys.: Condens. Matter* **2002**, *14*, 2745.
[50] V. Lubarda, *Mech. Mater.* **2003**, *35*, 53.
[51] L. J. Krayer, E. M. Tennyson, M. S. Leite, J. N. Munday, *ACS Photonics* **2018**, *5*, 306.
[52] L. Wang, Z. Zeng, C. Ma, Y. Liu, M. Giroux, M. Chi, J. Jin, J. Greeley, C. Wang, *Nano Lett.* **2017**, *17*, 3391.
[53] C. Zhu, Q. Shi, S. Fu, J. Song, H. Xia, D. Du, Y. Lin, *Adv. Mater.* **2016**, *28*, 8779.
[54] M. Valenti, A. Venugopal, D. Tordera, M. P. Jonsson, G. Biskos, A. Schmidt-Ott, W. A. Smith, *ACS Photonics* **2017**, *4*, 1146.
[55] S. Kim, H. Wakatsuchi, J. J. Rushton, D. F. Sievenpiper, *Appl. Phys. Lett.* **2016**, *108*, 041903.
[56] K. F. MacDonald, Z. L. Sámson, M. I. Stockman, N. I. Zheludev, *Nat. Photonics* **2009**, *3*, 55.

